PHYSICAL REVIEW B VOLUME 16, NUMBER 4 15 AUGUST 1977

Electrical and thermal transport measurements on semimetallic rare-earth sesquisulfides

Syed M. A. Taher
Department of Physics, Wichita State University, Wichita, Kansas 67208

John B. Gruber
Department of Physics, College of Science and Mathematics, North Dakota State University, Fargo, North Dakota 58102

(Received 18 March 1976; revised manuscript received 13 September 1976)

Measured values of ρ, R_H, α, and κ are reported on single-crystal samples of Nd_2S_3, Gd_2S_3, and Dy_2S_3 containing excess rare earth in the defect lattice structure. Measurements cover the temperature range between roughly 7 and 1000 K, and an excess rare-earth composition range between 0.1 and 0.7 wt%. Data can be interpreted in terms of the Cutler-Mott model modified for magnetic effects by von Molnár, Holtzberg, Penney, and their associates. Above 100 K, alloy scattering appears dominant. At lower temperatures the transport mechanism favors a hopping process for localized electrons in a magnetically ordered lattice.

INTRODUCTION

The rare-earth sesquisulfides R_2S_3 having the Th_3P_4 defect-type structure, have received increasing attention in recent years with particular interest centered on the thermoelectric, optical, and magnetic properties of these substances.[1-22] There are several reasons for such interest.

First of all, these particular sulfides, which may be written as

$$R_{3-x}V_xS_4 \quad (0 \leq x \leq \tfrac{1}{3}; \quad V_x, \text{ vacancy}), \tag{1}$$

can be synthesized so as to change continuously from metallic to insulating behavior with increasing vacancy concentration V_x, leading to a variety of cooperative effects such as superconductivity and ferromagnetism.[9] However, the Th_3P_4 defect-type structure is maintained throughout the entire solid solution range $R_2S_3 - R_3S_4$.[23-25]

When $x=0$ (R_3S_4), all cation sites are filled and the compounds are metallic with La_3S_4 exhibiting superconductivity and others becoming magnetically ordered at relatively high temperatures.[9] When $x=\frac{1}{3}$ (R_2S_3) the compounds are insulators with $\frac{4}{3}$ of the cation sites per unit cell vacant. Several of these compounds, such as Gd_2S_3, become magnetically ordered at low temperatures.[9,16-18] With such a relatively large number of vacancies in R_2S_3 ($\sim 10^{22}/cm^3$) it has been possible to vapor diffuse excess rare earth, bismuth, or tellurium into the material thus introducing large numbers of carriers into the lattice which drastically change the thermoelectric properties.[2,26,27] Several of these materials have been characterized as heavily doped semiconductors.[2,26]

Crystals of R_2S_3 grown from the melt containing slight excess metal are characterized as degenerate wide-band-gap n-type semiconductors.[2,6,9,16-19] Many of them exhibit magnetic ordering below liquid-nitrogen temperature. Along with RX, where $X=O$, S, Se, and Te, the doped R_2S_3 materials have become model substances for coordinated optical, magnetic, and thermoelectric experiments and serve as interesting models for ionic semiconductors.[8,16-20]

There still persists interest in raising the magnetic ordering temperature in these compounds through various doping experiments. Henderson, Gruber, and their co-workers have grown mixed rare-earth sesquisulfides such as Nd_2S_3-Gd_2S_3 with various dopants that provide magnetic ordering temperatures above 100 K.[27-29] However, these heavily doped magnetic semiconductors may have even greater potential as energy conversion devices operating above room temperature. Percent changes in excess doping change ρ by more than 10^{14} (ohm cm) and α by more than a factor of 10^4 at a given temperature, yet doping does not appear to change the lattice parameters appreciably,[27-29] nor do values of κ change by more than a factor of 10 over the range $0 \leq x \leq \frac{1}{3}$.[7,15,28]

The purpose of this communication is to report the thermoelectric measurements made by the authors between 7 and roughly 1000 K on slightly metal-rich single crystals of Nd_2S_3, Gd_2S_3, and Dy_2S_3 grown by Henderson, Gruber, and their coworkers at McDonnell-Douglas Astronautics Company in Santa Monica, California. We also hope to show that in accord with the conclusions of previous investigators we find that below and even somewhat above the magnetic ordering temperature the Cutler-Mott model[8] modified for magnetic interactions by von Molnár, Penney, Holtzberg, and their associates[16-18] does indeed prevail and that at higher temperatures the alloy scattering model of Taher, Gruber, and Olsen[19] associated with the tailed conduction-band model of Cutler and Mott[8] appears reasonable.

CRYSTAL PREPARATION AND GROWTH

Henderson, Gruber, and their co-workers prepared powders of the sesquisulfides of Nd, Gd, and Dy by passing either H_2S or CS_2 through pyrolitic graphite tubes containing the oxide (R_2O_3) at elevated temperatures.[6] Single crystals were grown from the powder using two different techniques: (i) by flame fusion in an argon plasma, and (ii) by the conventional Bridgman technique using an rf induction heater capable of reaching 2000 °C. Crucibles of pyrolytic graphite capped with a graphite lid were lowered through a melting zone inside a quartz water jacket in the presence of an atmosphere of dry inert gas. Many of the crystals grown were dark in color or black, and glossy on the surfaces. We found no evidence of carbide formation between crucible walls and molten material.

Wet-chemical analyses and neutron-activation analyses were carried out on samples taken from the same boule that supplied crystals for thermoelectric measurements. Since the starting R_2O_3 material was usually better than five-nines purity, only trace metal elements were found from neutron-activation analyses of the sesquisulfides. We found no evidence of oxygen in our samples, concluding that neither R_2O_3 nor the oxysulfides were present in the crystals. To learn if a composition or impurity gradient was present in a given boule, we called for wet-chemical analyses of material taken from the sample slices as well as from the ends of the boule. Within the uncertainty of the chemical analyses we found the boule to be homogeneous in composition. Excess metal content above R_2S_3 stoichiometry is as follows: $Nd_2S_3(1)$, 0.7% Nd; $Nd_2S_3(2)$, 0.6% Nd; $Gd_2S_3(1)$, 0.4% Gd; $Gd_2S_3(2)$, 0.5% Gd; $Dy_2S_3(1)$, 0.1%Dy; $Dy_2S_3(2)$, 0.2% Dy. Percentages are reported as excess weight percent, with a ±0.2% uncertainty associated with the chemical analyses.

Electron microscope photographs and x-ray Laue photographs were used to establish the crystal structure and orientation. We are able to select portions of the crystal having no observable strains or imperfections. X-ray studies confirmed the crystal structure to be the Th_3P_4 defect type as described by Meisel and Zachariasen.[30,31]

ELECTRICAL AND THERMAL TRANSPORT MEASUREMENTS

Slices approximately 1-mm thick were cut from the boule using a diamond saw. Sample bars approximately 6mm by 1.2 mm with six contact arms (two on each side 1.8 mm apart and two on the ends) were cut out of the slice by spark-machining. Sample bars were polished and cleaned with benzene and methyl alcohol. Contact pastes of silver and platinum fired gently onto the arms made good ohmic contacts for measurements below room temperature. For higher temperatures, ohmic contacts were made by sputtering thin platinum film onto highly polished and cleaned sample arms. Electrical contacts were made using tin-lead solder for low-temperature measurements and pressure contacts were used at temperatures above which this solder mixture failed. To measure the temperature we used a copper-iron gold thermocouple between 4.2 and 100 K, and a chromel-alumel thermocouple from 100 to 1000 K, with an ice-water bath as a standard.

To measure the thermoelectric power and thermal conductivity, both the sample and a half-watt resistor heater were mounted to a copper block in good thermal contact. The block could be mounted either to the liquid-helium conduction Dewar or to the high-temperature furnace. The value of ΔT could be measured to better than 5% as an average over many runs. We used standard methods to measure both the thermoelectric power and the thermal conductivity.[32] To measure the electrical transport properties such as ρ and R_H, we chose an AC method using an electronics system originally designed by Cunningham.[33] This method eliminated unwanted thermogalvanomagnetic effects. We were careful to avoid such spurious causes of anomalous Hall behavior such as surface effects and the Nernst-Ettinghausen effect. Hall measurements were made using a 4-in. Varian electromagnet with a field-regulated power supply that produced magnetic fields up to 7500 G with a regulation of 1×10^{-6} and field accuracy of 0.02%.

Between 4.2 and 300 K, measurements were made by allowing the sample in the liquid-helium conduction Dewar of standard design to warm up slowly enough so as to make measurements reproducible to better than 5% over several runs. Above 300 K, measurements were made by slowly raising the furnace temperature and repeating the measurements as closely as possible as the temperature was slowly lowered back to room temperature. Because of radiation losses and other experimental difficulties encountered, we finally decided to design and build our own furnace for high-temperature thermoelectric transport measurements which is described in the next paragraph and shown in Figs. 1(a), 1(b), 1(c), 1(d).

The furnace is designed so that the interior, including the heating elements, sample block and sample are all evacuated to better than 10^{-5} Torr. The outside jacket [see Fig. 1(a)] is made with stainless steel and has nonmagnetic tubing coiled about the outside wall keeping the outside reason-

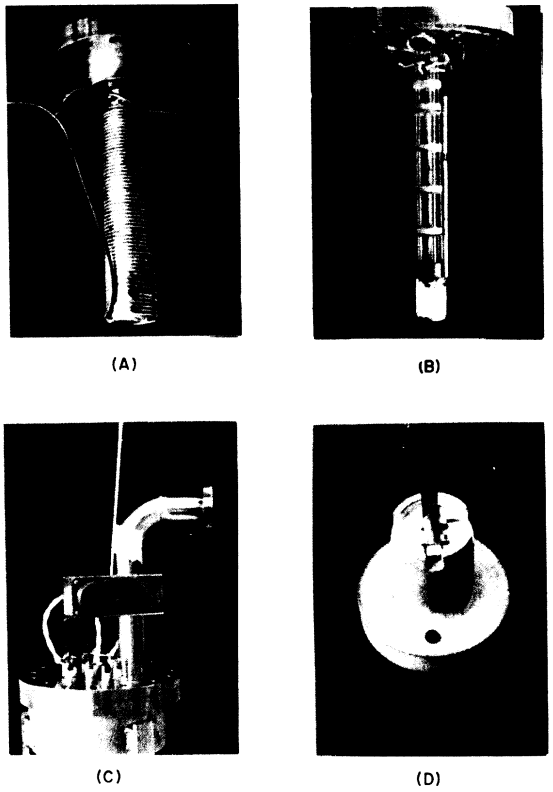

FIG. 1. High-temperature furnace apparatus used to measure transport properties. See text for description of parts A, B, C, and D.

ably cool. The inside of the outer jacket is treated to cut down on radiation losses. The interior frame [see Fig. 1(b)] consists of four vertical quartz rods that support the entire furnace assembly and are held in vertical position by ceramic spacers. The frame is supported by a stainless-steel flange that can be screwed into the top flange. The ceramic spacers also allow thin quartz tubing containing the leads to pass through on their way from the top flange to the heater assembly and sample block. Care was taken to shield sample leads from electrical leads and thermal gradients. The main body of the furnace located at the bottom of the frame in Fig. 1(b) consists of six vertical tungsten pins which act as voltage probes, three lava disks used to hold the pins in position, a hollow heating furnace constructed of lava having tantalum (tungsten) wire as the heating element, and a sample holder made of lava which fits smoothly up into the furnace from the bottom and is held in place with molyscrews. Figure 1(c) shows the top flange with pumping neck and feedthroughs for all leads, and Fig. 1(d) shows the sample block assembly. The sample sits nearly inside the middle of the furnace with the sample block containing the sample and the resistor heater, so orientated that a controlled ΔT can be established through differential heating between the furnace and the resistor.

ELECTRICAL AND THERMAL TRANSPORT DATA

Electrical resistivity (ρ), absolute value of the Hall coefficient (R_H), absolute value of the thermoelectric power (α), and the thermal conductivity coefficient (κ) measured as a function of absolute temperature are presented in Figs. 2–5 for two different samples each of Nd_2S_3, Gd_2S_3, and Dy_2S_3 with excess rare earth as indicated earlier.

We have found, as did von Molnár, Holtzberg, and their associates, that the magnetic properties of these n-type semiconductors cannot be ignored in the interpretation of the low-temperature electrical transport data.[16-18] We asked Beeler in our group to measure the magnetic susceptibility and magnetic moments as a function of temperature and magnetic field using powdered samples taken from single crystals similar to those used for our transport measurements.[34] This past summer the authors also had an opportunity to confirm and extend these magnetic measurements. It is clear that both Nd_2S_3 and Gd_2S_3 become magnetically ordered around 60 and 30 K, respectively, in the samples reported here with the following magnetic parameters: Nd_2S_3, $C_M = 1.38$, $\theta = 61.1$; Gd_2S_3, $C_M = 7.39$, $\theta = 39.0$; and Dy_2S_3, $C_M = 13.10$, $\theta = 8.9$. Graphs of $1/\chi_m$ vs K for all three materials, however, show a decided break near 100 K from an otherwise classical paramagnetic behavior above this temperature.[22] This same temperature also represents a minimum for all six samples in the electrical resistivity curves shown in Fig. 2.

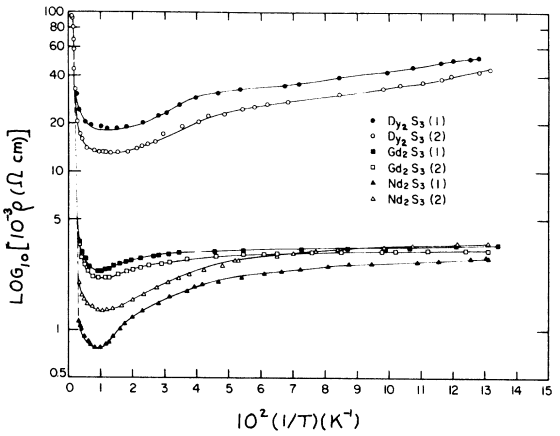

FIG. 2. Log of the electrical resistivity [$10^{-3}\rho$ (ohm-cm)] vs the reciprocal of the absolute temperature for samples described in text. Temperature range includes roughly 7–1000 K.

The higher magnetic ordering temperatures for Nd_2S_3 and Gd_2S_3 reported here and by Beeler and Gruber[22] are due to somewhat greater excess rare earth than found in samples studied by Adamyan *et al.*[4] for Nd_2S_3 and by Penney *et al.*[18] for Gd_2S_3.

In Fig. 2 between the minimum in resistivity near 100 K and θ we have determined the following activation energy E_a, for each sample as measured down from the minimum edge of the conduction band where $E_a = E_c = 0$ eV. The energies are: $Nd_2S_3(1)$, $E_a = -3.86 \times 10^{-3}$ eV; $Nd_2S_3(2)$, $E_a = -2.70 \times 10^{-3}$ eV; $Gd_2S_3(1)$, $E_a = -1.93 \times 10^{-3}$ eV; $Gd_2S_3(2)$, $E_a = -1.60 \times 10^{-3}$ eV; $Dy_2S_3(1)$, $E_a = -1.58 \times 10^{-3}$ eV; and $Dy_2S_3(2)$, $E_a = -1.53 \times 10^{-3}$ eV. These activation energies are comparable to values reported for $Ce_{3-x}V_xS_4$ by Cutler and Leavy[2] and for $Gd_{3-x}V_xS_4$ by von Molnár *et al.*[16] Below θ, the resistivity remains activated but shows increasingly less activation from Nd_2S_3 to Gd_2S_3 to Dy_2S_3. Below 20 K, the resistivity is essentially constant for all samples. We have not as yet carried out resistivity measurements as a function of magnetic field. However, we expect to observe a negative magnetoresistance as von Molnár *et al.* have reported for Gd_2S_3.[16-18]

Above 100 K and extending to nearly 1000 K for $Dy_2S_3(2)$ we find the resistivities increasing as shown in Fig. 2. The increase in resistivity shows similar behavior to that observed for $Ce_{3-x}V_xS_4$ for similar excess rare-earth content.[2] Near 1000 K the resistivity for $Dy_2S_3(2)$ apparently reaches a maximum. Above 1200 K Henderson, Gruber, and their co-workers found for similar Dy_2S_3 samples that ρ began to decrease very rapidly as they apparently had reached the intrinsic region.[6] From the slope of their data above 1200 K an activation energy of about -2.1 eV can be deduced. Optical reflectivity spectra on doped Dy_2S_3 and transmission spectra of stoichiometric Dy_2S_3 suggest a band gap between 5700 and 4800 Å or between -2.18 and -2.58 eV.[35] Additional reflectivity studies are planned.

In Fig. 3, we report the absolute value of the measured Hall coefficient against the reciprocal of the absolute temperature for all six samples. Measurements were made between roughly 7 and 300 K for all samples except $Dy_2S_3(2)$ where we were able to reach 600 K. At higher temperatures the sign of the Hall coefficient is negative. With decreasing temperature the magnitude of the coefficient decreases to around 100 K and shows an anomalous peak in Fig. 3 around 20 K before dropping down to a constant value between roughly 13 and 7 K. We have assured ourselves that such results are not spurious.

To determine meaningful carrier concentrations

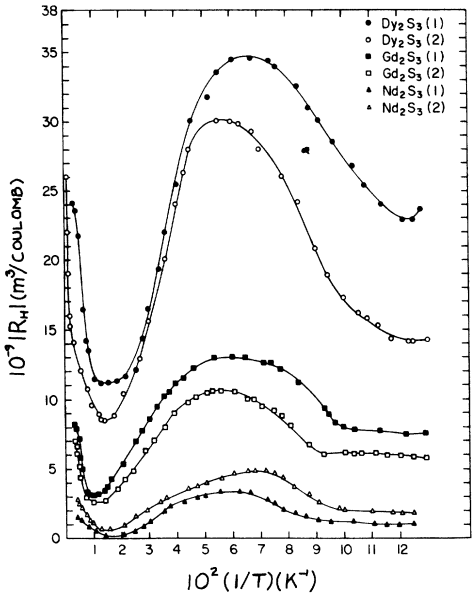

FIG. 3. Measured value of the Hall coefficient $[10^{-9}|R_H|(m^3/\text{coulomb})]$ vs the reciprocal of the absolute temperature for samples described in text. Temperature range includes roughly 7–600 K.

and mobilities from these data, particularly below 100 K, we need to separate the anomalous from the normal Hall coefficient. We have followed a method of analysis suggested by Shapira and Reed[36] and by von Molnár and Holtzberg.[17] The method involves plotting the measured Hall coefficient as a function of magnetic susceptibility χ, using the functional form,

$$R_H = R_{H(0)} + [(4\pi - N)R_{H(0)} + R_{H'}]\chi^*, \tag{2}$$

where $R_{H(0)}$ and $R_{H'}$ are the normal and anomalous Hall coefficients and N is the demagnetizing factor. Above approximately 85 K we find essentially a linear relationship for R_H vs $\chi^* \approx \chi$ which allows us to find $R_{H(0)}$ from the intercept. Values for carrier concentration n are calculated from the magnitude of $R_{H(0)}$ determined in this way. We express n as

$$n \equiv \lim_{\chi \to 0} \left(\frac{1000 B r}{e|R_H|} \right) \text{cm}^{-3}, \tag{3}$$

where r is a function of the scattering mechanism and degree of degeneracy and B depends on the band structure. Previous work has shown that Br is independent of temperature and somewhat less than unity for the parabolic band model with alloy scattering.[19,28] At 300 K we obtain the following carrier concentrations n, for the following sam-

ples: $Nd_2S_3(1)$, $(3.6\pm0.2)\times10^{21}/cm^3$; $Nd_2S_3(2)$, $(2.0\pm0.3)\times10^{21}/cm^3$; $Gd_2S_3(1)$, $(5.0\pm0.3)\times10^{20}/cm^3$; $Gd_2S_3(2)$, $(7.6\pm0.2)\times10^{20}/cm^3$; $Dy_2S_3(1)$, $(2.5\pm0.2)\times10^{20}/cm^3$; and $Dy_2S_3(2)$, $(3.9\pm0.2)\times10^{20}/cm^3$.

These values appear reasonable when compared with known excess rare earth and measured sample densities and masses. Furthermore, the high-temperature results are consistent with the transport behavior found for $Ce_{3-x}V_xS_4$. All our samples have carrier concentrations over $\sim10^{20}/cm^3$ and exhibit degenerate semiconductor behavior over the same temperature range covered by Cutler and Leavy.[2] Since the Hall mobility is not constant over temperature, values of n_∞ (value of n as $1/T\to0$, μ = constant) cannot be determined easily, but we can compare our values of n for $Gd_2S_3(1)$ and (2) with values reported by von Molnár *et al.* and Penney *et al.*[16-18] In Table I of Ref. 17 n_∞, μ and ρ at room temperature, and $\theta(K)$ are given. Values of n_∞ and $\theta(K)$ increase with samples more heavily doped with excess rare earth. Our results for n and $\theta(K)$ are somewhat higher than similar values in Ref. 17 which is expected since our samples are more heavily doped with excess rare earth.

In Fig. 4 the absolute value of the thermoelectric power is plotted against the absolute temperature. The sign of α is negative over the entire temperature range (7 to 1000 K). The value of $|\alpha|$ is a linear function of K for all samples from approximately 120 K to nearly 800 K for $Dy_2S_3(2)$. The only measurements made so far below 100 K are for the Gd_2S_3 samples which show minima around 80 K, which rise to a maxima somewhat above θ, and then approach 0 as the temperature approaches zero. This behavior is similar to that reported by von Molnár and his associates for Gd_2S_3.[16,18] We suspect that the Dy_2S_3 and Nd_2S_3 samples may show similar behavior at lower temperatures as well. We are planning to carry out low-temperature measurements for $|\alpha|$ on similar Dy_2S_3 and Nd_2S_3 samples in the near future. We have found the explanation given by von Molnár *et al.* and by Penney *et al.* to be satisfactory in explaining our $|\alpha|$ data below 100 K for Gd_2S_3, but we hesitate to postulate the same explanation for our other samples until $|\alpha|$ has been measured for them below 100 K.

Above 800 K for $Dy_2S_3(2)$ we find $|\alpha|$ beginning to level off which makes us suspect we have reached a maximum value between 900 and 1000 K. Henderson, Gruber, and their co-workers[6,35] found for similar Dy_2S_3 crystals that $|\alpha|$ reached a maximum at approximately 1000 K and began to decrease rapidly from 1200 to 1400 K. At 1000 K for $Dy_2S_3(2)$ α has a value of -350 μV/K; we have estimated that at the same temperature for $Dy_2S_3(1)$ α will have a value of around -500 μV/K. Doping experiments have shown that $|\alpha|$ and ρ can be changed by judicious choice of dopants. However, ρ changes much more drastically than $|\alpha|$. Future plans call for extending measurements of $|\alpha|$ vs K

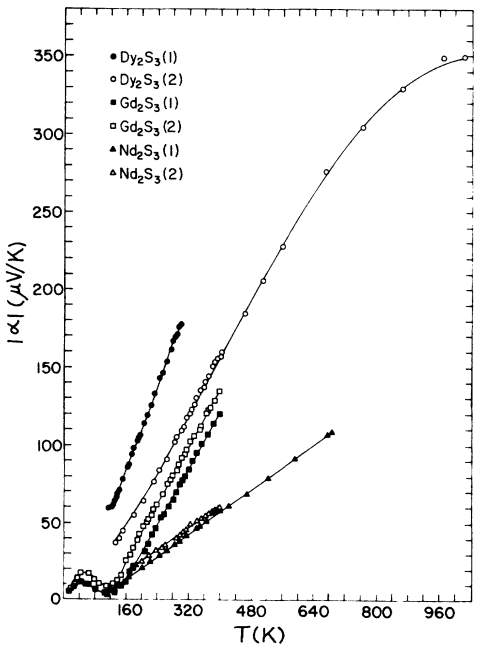

FIG. 4. Measured values of the thermoelectric power (Seebeck coefficient) $|\alpha|(\mu V/K)$ vs the absolute temperature for samples described in text.

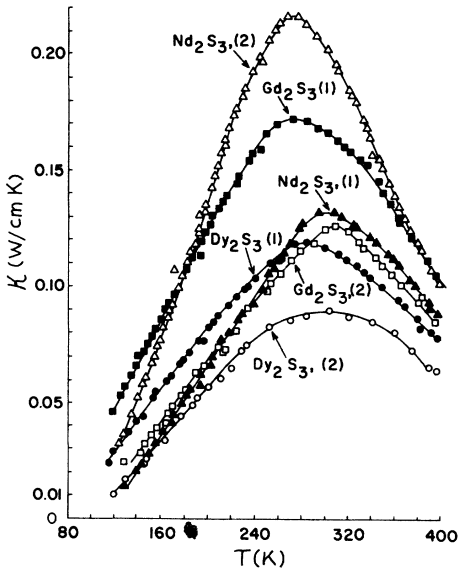

FIG. 5. Measured values of the thermal conductivity κ(W/cm K) vs the absolute temperature for samples described in text.

to additional samples.

Figure 5 includes values of the thermal conductivity (κ) between 100 and 400 K. The thermal conductivities for all samples reach their maximum value between 280 and 300 K. Maximum values are separated by a factor of 2.5 between the extremes of $Nd_2S_3(2)$ and $Dy_2S_3(2)$. However, as we move further away from the maxima the values of κ for all samples become more nearly the same. Isolated measurements of κ on similar Dy_2S_3 samples at 600 and 800 K give values of 0.01 and 0.008 W/cm K respectively. We expect that κ for our Nd_2S_3 and Gd_2S_3 samples will decrease in the same fashion at higher temperatures although their values will be somewhat higher. Goryachev and Kutsenok[7] report values of $\kappa = 0.012$ and 0.008 W/cm K at temperatures 300 and 1200 K for Ce_2S_3. For increased rare-earth content they show an increase in κ which is similar to values reported here. Values of κ are also reported in Ref. 15 for La_3S_4 where an effort was made to interpret the data.

It is evident in Fig. 5 that above 300 K the decreasing thermal conductivity may be ascribed to the dominant contribution from the phonons to the total thermal conductivity. The increase in κ at 300 K with increasing excess rare earth in going from Dy_2S_3 to Gd_2S_3 to Nd_2S_3 may be due to a reduction in the anharmonicity of the lattice vibrations because of the gradual filling of vacancies in the $R_{3-x}V_xS_4$ sublattice. Below 300 K the decrease in κ can be ascribed to several mechanisms including carrier, defect and impurity scattering.[8,32,37]

COMMENTS

The model developed by Cutler and Mott and extended to magnetic degenerate semiconductors by von Molnár, Holtzberg, Penney, and their associates appears to explain our data as well.[8,16-18] The model assumes a random distribution of cation vacancies that contribute fluctuating repulsive potentials and consequent tailing of the conduction band in which the electronic states are localized. A bound magnetic polaron model appears to interpret the transport data for magnetically ordered Gd_2S_3 below 100 K. The rigid band model appears reasonable for the semimetallic samples we report here since the donor concentration is still comparable to the more heavily doped $Ce_{3-x}V_xS_4$ samples reported by Cutler and Leavy.[2]

We have reported earlier on a parabolic band model calculation with consideration for acoustical phonon, charged impurity, lattice and alloy scattering and have given expressions for σ, α, and τ for each scattering mechanism.[19,28] Based on the alloy scattering model, the low-temperature Fermi energy determined from the $|\alpha|$ data in Fig. 4 lies within the conduction band for all samples. Thus at low temperatures the model predicts that conduction occurs in extended states and remains finite as the temperature approaches zero. This is indeed the case as observed in Fig. 2. The model also predicts the linear nature of $|\alpha|$ with temperature down to nearly 100 K with an extrapolated nonzero intercept and with decreasing slope with increasing carrier concentration. Again, this is observed for $|\alpha|$ in Fig. 4 except for Gd_2S_3 below 80 K for which we follow the analysis of Penney *et al.*[18] and above 800 K where other mechanisms dominate near the intrinsic region.[28]

Rather than repeat in detail our method of analysis of data in Figs. 2–4 which we have described earlier,[19,28] we will simply state the general approach and our results. We have compared experimental ratios of $\rho(T)/\rho(300\text{ K})$ and $\mu(T)/\mu(300\text{ K})$ plotted against the absolute temperature with the same ratios predicted for the various scattering models. Values of μ were determined using the normal Hall coefficient as determined earlier. Above 100 K, alloy scattering appears to dominate.

An earlier determination based on alloy scattering has shown that values of m^*/m are reasonably independent of temperature above 100 K for samples reported here with an average value at 140 K of approximately 1.9 for Gd samples, 3.8 for Nd samples and 3.4 for Dy samples.[28] Cutler and Leavy[2] have used a value of 3.1 to interpret their data for Ce samples, and von Molnár and Holtzberg[17] used 1.6 for Gd samples. The comparisons made here involve samples of carrier concentrations greater than $\sim 10^{20}/\text{cm}^3$. Below 100 K, magnetic effects cannot be ignored. Likewise the predicted scattering distances including magnetic effects in the scattering term suggest that below 100 K we are getting into a range where the transport mechanism is a hopping process for localized electrons. The low-temperature $|\alpha|$ data in Fig. 4 support this conclusion. As a general concluding remark, we find that our data can be interpreted along the lines suggested earlier for other rare-earth sesquisulfides containing excess rare earth in the defect lattice.

ACKNOWLEDGMENTS

Many of the data reported here were taken at Washington State University. Neutron activation analyses of samples were also carried out at WSU. Financial support for these studies at WSU was provided in part under ERDA contract AT(45-1)-2221-T6. The authors also wish to express appreciation to Dr. L.C. Olsen, Joint Center for

Graduate Study, Richland, Washington, for his help while the authors were at WSU. We wish to thank R. Z. Bachman and G. V. Austin, Ames Laboratory, Iowa State University, for checking earlier chemical analyses of samples. Also one of us (JBG) wishes to express his appreciation to Professor K. A. Gschneidner, Jr., Professor D. W. Lynch, and staff members B. J. Beaudry and H. R. Shanks, Ames Laboratory, ISU, for helpful discussions, assistance, and use of experimental apparatus for checking and completing some experimental details for this manuscript.

[1]M. Cutler, R. L. Fitzpatrick, and J. F. Leavy, J. Phys. Chem. Solids 24, 319 (1963).
[2]M. Cutler and J. F. Leavy, Phys. Rev. 133, A1153 (1964).
[3]R. M. Bozorth, F. Holtzberg, and S. Methfessel, Phys. Rev. Lett. 14, 952 (1965); see also F. Holtzberg and S. Methfessel, J. Appl. Phys. 37, 1433 (1966).
[4]V. E. Adamyan, A. V. Golubkov, G. M. Loginov, and V. N. Fedorov, Fiz. Tver. Tela 7, 3372 (1965) [Sov. Phys.-Solid State 7, 2715 (1966)].
[5]V. E. Adamyan and G. M. Loginov, Zh. Eksp. Teor. Fiz. 51, 1044 (1966) [Sov. Phys.-JETP 24, 696 (1967)].
[6]J. R. Henderson, M. Muramoto, E. Loh, and J. B. Gruber, J. Chem. Phys. 47, 3347 (1967).
[7]Goryachev and T. G. Kutsenok, Fiz. Tekh. Poluprovodn. 3, 277 (1969) [Sov. Phys.-Semicond. 3, 230 (1969)].
[8]M. Cutler and N. F. Mott, Phys. Rev. 181, 1336 (1969).
[9]*Landolt-Börnstein, Group III, 4a,* edited by K. H. and A. M. Hellwege, Part 2 prepared by F. Holtzberg, T. R. McGuire, and S. Methfessel, pp. 90–94 (1970).
[10]V. P. Zhuze, V. M. Sergeeva, and O. A. Golikova, Fiz. Tver. Tela 11, 2568 (1969) [Sov. Phys.-Solid State 11, 2071 (1970)].
[11]J. R. Henderson, M. Muramoto, J. B. Gruber, and E. R. Menzel, J. Chem. Phys. 52, 2311 (1970).
[12]A. T. Starovoĭtov, V. I. Ozhogin, G. M. Loginov, and V. M. Sergeeva, Zh. Eksp. Teor. Fiz. 57, 791 (1969) [Sov. Phys.-JETP 30, 433 (1970)].
[13]V. I. Novikov and S. S. Shalyt, Fiz. Tver. Tela 12, 3252 (1970) [Sov. Phys.-Solid State 12, 2628 (1971)].
[14]G. M. Loginov, V. M. Sergeeva, and M. F. Bryzhina, Fiz. Tver. Tela 12, 3620 (1970) [Sov. Phys.-Solid State 12, 2942 (1971)].
[15]V. P. Zhuze, O. A. Golikova, V. M. Sergeeva, and I. M. Rudnik, Fiz. Tverd. Tela 13, 811 (1971) [Sov. Phys.-Solid State 13, 669 (1971)].
[16]S. von Molnár, F. Holtzberg, T. R. McGuire, and T. J. A. Popma, AIP Conf. Proc. 5, Magnetism and Magnetic Materials, 869 (1972).
[17]S. von Molnár and F. Holtzberg, AIP Conf. Proc. 10, Magnetism and Magnetic Materials, 1259 (1973).
[18]T. Penney, F. Holtzberg, L. J. Tao, and S. von Molnár, AIP Conf. Proc. 18, Magnetism and Magnetic Materials, 908 (1974).
[19]S. M. A. Taher, J. B. Gruber, and L. C. Olsen, J. Chem. Phys. 60, 2050 (1974).
[20]O. A. Golikova and I. M. Rudnik, Fiz. Tekh. Poluprovodn. 8, 1825 (1974) [Sov. Phys.-Semicond. 8, 1186 (1975)].
[21]D. G. Andrianov, G. P. Borodulenko, A. A. Grizik, S. A. Drozclov, and V. I. Fistul', Fiz. Tverd. Tela 17, 1831 (1975) [Sov. Phys.-Solid State 17, 1199 (1975)].
[22]H. D. Beeler and J. B. Gruber, Chem. Phys. 13, 359 (1976).
[23]M. Picon, L. Domange, J. Flahaut, M. Guittard, and M. Patrie, Bull. Soc. Chim. Fr. 2, 221 (1960).
[24]J. Flahaut, M. Guittard, and M. Patrie, Bull. Soc. Chim. Fr., Paper No. 180, 990 (1958).
[25]G. V. Samsonov and S. V. Radzikovskaya, Ukr. Khim. Zh. 26, 421 (1960).
[26]Compositions for X between 0 and $\frac{1}{3}$ in Eq. (1) are described in various Refs. 1–22. However, efforts to dope with other than rare earths (such as Bi and Te) have been reported by J. B. Gruber, USAEC Progress Reports, RLO-2221-T6-13A, 15-C, and 20-C (1972–1974) (unpublished).
[27]J. R. Henderson, M. Muramoto, E. Loh, and J. B. Gruber, Bull. Am. Phys. Soc. II 14, 310 (1969).
[28]J. B. Gruber, USAEC Progress Reports, RLO-2221-T6-13 (1972); RLO-2221-T6-15 (1973); and RLO-2221-T6-20(REV)(1974) (unpublished).
[29]J. R. Henderson *et al.*, U. S. Patent No. 3,748,095 (July, 1973), owned by McDonnell-Douglas Corp., Long Beach, Calif. 90846.
[30]K. Meisel, Z. Anorg. Chem. 240, 300 (1939).
[31]W. H. Zachariasen, Acta Cryst. 2, 57 (1949).
[32]H. J. Goldsmid, *Thermoelectric Refrigeration* (Plenum, New York, 1964).
[33]R. W. Cunningham, Ph.D. thesis (Washington State University, 1969), (unpublished).
[34]H. L. Beeler, Ph.D. thesis (Washington State University, 1975), (unpublished).
[35]J. R. Henderson and J. B. Gruber (unpublished).
[36]Y. Shapira and T. B. Reed, Phys. Rev. B 5, 4877 (1972).
[37]J. M. Ziman, *Principles of the Theory of Solids,* (Cambridge U. P., Cambridge, England, 1969).

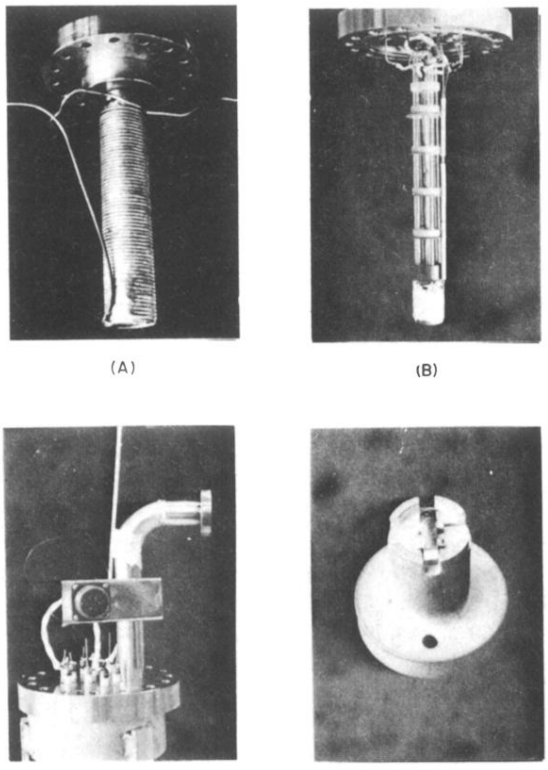

FIG. 1. High-temperature furnace apparatus used to measure transport properties. See text for description of parts *A*, *B*, *C*, and *D*.